J. Phys. B: At. Mol. Opt. Phys. **32** (1999) R39–R65. Printed in the UK PII: S0953-4075(99)94044-0

**TOPICAL REVIEW**

# Hollow atoms

Hannspeter Winter† and Friedrich Aumayr

Institut für Allgemeine Physik, Technische Universität Wien, Wiedner Hauptstraße 8-10, A-1040 Wien, Austria

Received 1 December 1998

**Abstract.** The 'hollow atom' (HA) is the latest and probably most exotic creation of atomic collision physics. HA are short-lived multiply-excited neutral atoms which carry a large part of their $Z$ electrons ($Z$, the projectile nuclear charge) in high-$n$ levels while inner shells remain transiently empty. This population inversion arises for typically 100 fs during the interaction of a slow highly charged ion with a solid surface. Despite this limited lifetime, the formation and decay of a HA can be conveniently studied from ejected electrons and soft x-rays, and the trajectories, energy loss and final charge state distribution of surface-scattered projectiles. For impact on insulator surfaces the potential energy contained by HA may also cause the release of target atoms and ions. This topical review gives a short historical account of relevant experimental methods and studies in this field, presents a now widely accepted scenario for HA formation and decay, discusses some results from recent studies of the authors and concludes with an outlook on open questions and further promising aspects in this new field of atomic collisions.

## 1. Introduction

Bombardment of solid surfaces by fast neutral or ionized atoms and molecules has been of continuous interest for more than a hundred years because of its many important technical applications. In the majority of such applications only the kinetic projectile energy is of importance as, e.g., for particle-induced electron emission, ion scattering and sputtering. However, some ion-induced phenomena depend on the internal (potential) projectile energy, particularly if this potential energy greatly exceeds the kinetic projectile energy. In a highly charged ion (HCI), potential energy will be stored according to its production where $q$ electrons ($q$, the ion charge state) have to be removed from an originally neutral atom, and this potential energy becomes very large for high values of $q$ as shown in figure 1. Upon surface impact this potential energy is available for inducing various inelastic processes while the HCI will regain its $q$ missing electrons to again become fully neutralized. The HCI deposits its potential energy in a short time (typically about 100 fs) within a small area (typically less than 1 nm$^2$). In the course of HCI neutralization at the surface, according to our present knowledge a multiply-excited neutral particle with empty inner shells is formed.

The term 'hollow atom' (HA) appears to have first been coined by Briand *et al* (1990) in an account on projectile-characteristic soft x-ray emission resulting from impact of 340 keV $Ar^{17+}$ on a gas-covered silver surface. Now it is believed that such x-rays are emitted in the late stage of HA decay at and below the surface. On the other hand, a large number of slow electrons can have been already emitted before a HA has touched the surface. Therefore HA of the (1) and (2) kind have been defined, and some other distinctions have also been introduced to

† Author to whom correspondence should be addressed. E-mail address:winter@iap.tuwien.ac.at

0953-4075/99/070039+27$19.50 © 1999 IOP Publishing Ltd 

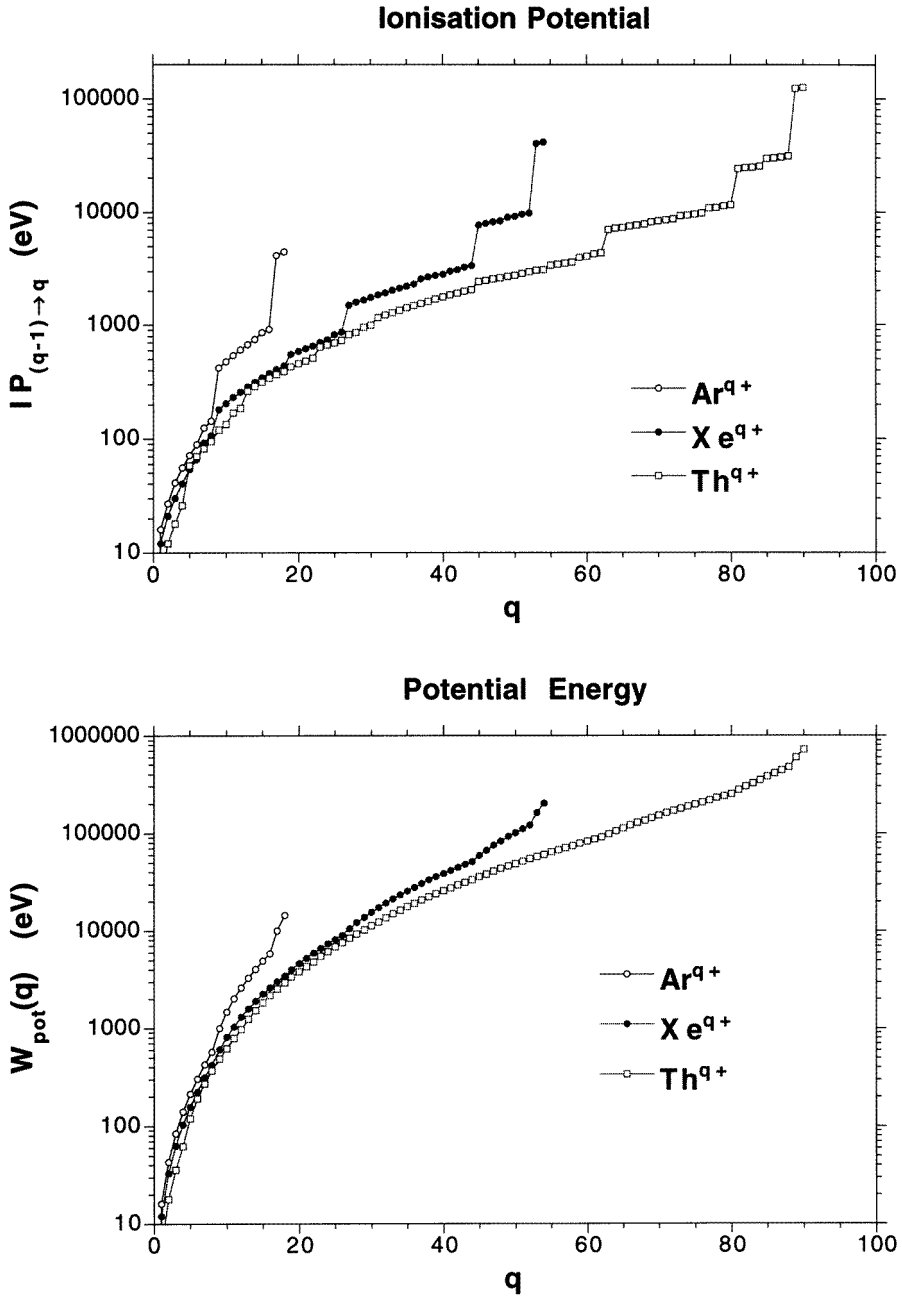


**Figure 1.** Ionization energies $\mathrm{IP}_{(q-1)_q}$ and total potential energy $W_{\mathrm{pot}}(q)$ of $\mathrm{Ar}^{q+}$, $\mathrm{Xe}^{q+}$ and $\mathrm{Th}^{q+}$ ions versus their charge state $q$ (data calculated after Mau 1990).

clarify the complete scenario of HA formation and decay. We remark that the term HA is also used for quite different systems such as, e.g., multiply-excited atoms produced by energetic synchrotron radiation (Kiernan *et al* 1994) or multiphoton absorption (Moribayashi *et al* 1998), but such HA are not the subject of this review.

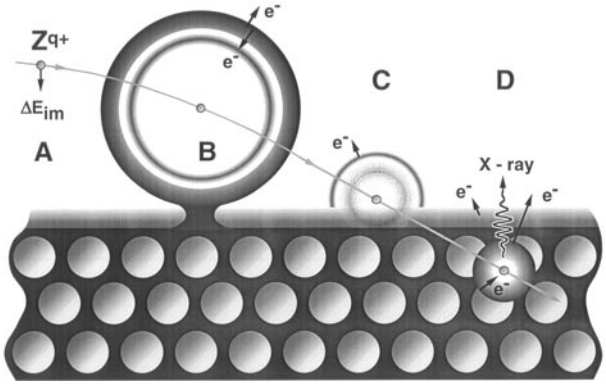


**Figure 2.** Scenario for impact of a slow HCI on a metal surface. (*a*) The HCI approaches the surface by acquiring image-charge energy gain $\Delta E_{im}$; (*b*) formation of HA above the surface gives rise to autoionization; (*c*) screening of the HA by surface electrons causes further electron emission; (*d*) relaxation of the HA at/below the surface proceeds by electron and x-ray emission.

HCI can be produced by powerful ion sources for virtually all chemical elements $Z$ and charge states $q$, and one can easily realize situations where the kinetic energy of a HCI becomes much smaller than its internal (potential) energy. For example, removing 80 electrons from neutral thorium ($Z = 90$), i.e. creating a very highly charged (neon-like) $Th^{80+}$ ion, requires an energy of about 250 keV (see figure 1), which will be reclaimed upon impact of this HCI on a solid surface. Ions with kinetic energies of a few keV can conveniently be transported through an experimental apparatus, but for HCI such experiments require ultra-high vacuum conditions in order to prevent partial HCI recombination in collisions with background gas molecules. Furthermore, the electronic and topographic status of the applied solid surfaces strongly influence both the nature and strength of its interaction with HCI, as is true for all potential energy-driven effects in particle–surface collisions.

Ground-breaking studies on slow ion–solid interaction were conducted by H D Hagstrum at Bell Laboratories (USA) and by U A Arifov and co-workers in Tashkent (Usbekhistan—former USSR) in the 1950s and 1960s. These studies showed that electron capture from a clean metal surface into a slowly approaching ion gives rise to Auger electron transitions where two or more electrons interact via their Coulomb repulsion, which can result in electron ejection into vacuum. The reason for this electron emission is the ion potential energy (see above). A HCI can capture many electrons into comparably high $n$-shells from a surface within a short time, thereby producing a multiply-excited neutral particle, i.e. a HA. Such HA are subject to rapid de-excitation by way of autoionization and thus emission of a number of slow electrons. For example, impact of a slow $Th^{80+}$ ion on a clean gold surface produces the tremendous amount of more than 300 electrons (Aumayr *et al* 1993), see section 4. Such electron emission has been investigated together with other experimental signatures such as the trajectory, charge state and kinetic energy loss of projectiles scattered on flat single-crystalline target surfaces, and the emission of projectile-characteristic fast Auger electrons and soft x-rays. The expertise thereby collected has led to our present understanding of the transient formation and decay of HA, which can be characterized by the scenario shown in figure 2.

Stages (A) and (B) of this scenario can be described within a so-called 'classical over-the-barrier model', COB model (see section 3). As soon as the HA closely approaches the surface (stage C), it becomes screened by the metal electron gas which causes further accelerated de-excitation.

Finally, in stage D all remaining inner shell vacancies will be filled, which gives rise to emission of fast Auger electrons and/or soft x-rays, depending on the projectile fluorescence yield. It is important to note that these different de-excitation processes can neither be precisely distinguished from each other nor clearly separated in time. For example, fast Auger electron emission can start in stage B and slow electron emission can still arise during stage D. However, as will be explained in section 2, slow electron emission yields and multiplicities deliver information particularly on the above- and at-surface stages B and C, whereas from spectra of fast Auger electrons and soft x-rays, details on the HA configuration at and below the surface (stages C and D) can be obtained.

In section 2 we will briefly present the most relevant experimental evidence for HA formation and decay, and in section 3 the theoretical background for our present understanding of the processes indicated in figure 2 will be provided. In section 4 we discuss our own recent work on HA-related phenomena, and then conclude with an outlook on some presently open questions and interesting aspects in this novel branch of atomic collision physics.

## 2. Experimental evidence for hollow atoms

In section 1 we briefly outlined our current view on HA formation from HCI impact on a solid surface. Now we will review the pertinent experimental methods and available experimental evidence for HA decay processes. A fairly complete account of this subject has recently been given by Arnau *et al* (1997).

Potential electron emission (PE) due to impact of slow singly, doubly and multiply charged ions on atomically clean metal surfaces has been thoroughly studied by Hagstrum (1953, 1954a, b, 1956). Figure 3(*a*) sketches Hagstrum's experimental set-up with which he measured the yields and energy distributions of ion-induced slow electrons. These studies showed that PE arises from relatively fast electronic transitions (rates $\geqslant 10^{14}$ s$^{-1}$) from the surface into empty projectile ion states, which require no minimum impact velocity and already start before an ion has entered the surface selvedge. PE yields increase strongly with the projectiles' potential energy or, more roughly speaking, their charge state. At higher impact velocity kinetic electron emission (KE) will also produce slow electrons which cannot be simply distinguished from the ones due to PE. Based on theoretical studies on 'radiationless' electronic transitions between a metal surface and a slow ion or excited atom by Massey (1930, 1931), Oliphant and Moon (1930), Shekter (1937) and Cobas and Lamb (1944), Hagstrum identified four one- and two-electron transitions (a)–(d) as being relevant for PE.

(a) *Resonant neutralization* (RN) transfers an electron from the surface into unoccupied states of the approaching ion which overlap filled surface valence band states. RN cannot give rise to electron emission but can be the precursor for subsequent electron emitting transitions (see below). Arifov *et al* (1973) noted that for HCI impact a sequence of RN processes can take place, which generates a short-lived multiply-excited particle, i.e. the HA of our present interest.

(b) *Resonant ionization* (RI) is inverse to RN and transfers an electron from the projectile into an empty surface state with a binding energy less than the surface work function $W_\phi$.

(c) *Auger neutralization* (AN, sometimes named *Auger capture*) can cause electron ejection from the surface valence band if the available potential energy exceeds twice $W_\phi$. One surface electron is captured by the ion and another one ejected with a kinetic energy $E_e \leqslant W_i' - 2W_\phi$. The respective electron energy distribution corresponds to a self-convolution of the surface electronic density of states (S-DOS).

(d) *Auger de-excitation* (AD) of the projectile occurs if the latter, after an RN or AN transition, carries excitation energy still larger than $W_\phi$. The excited projectile electron interacts

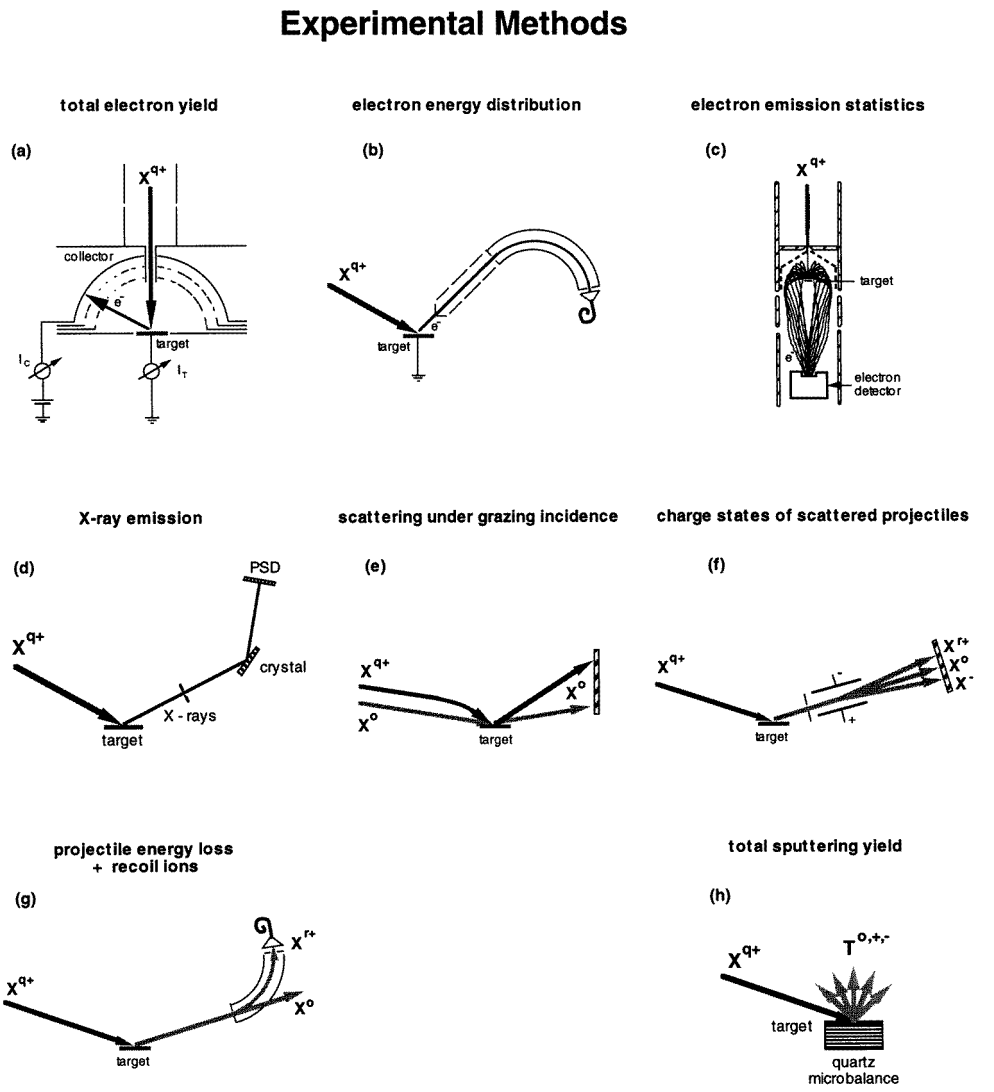


**Figure 3.** (*a*) Experimental set-up used by Hagstrum (1954a) for measuring total electron yields and ejected-electron energy distributions for ion-induced potential electron emission from atomically clean metal surfaces. (*b*) Typical experimental arrangement for Auger electron spectroscopy performed in HCI–surface interaction experiments. (*c*) Experimental set-up for measuring slow electron multiplicity distributions from slow HCI–surface impact. Electrons ejected from the target are accelerated to about 25 keV and guided into a surface barrier detector for measuring the pulse-height distributions. (*d*) Experimental set-up for high-resolution x-ray spectroscopy in HCI–surface interaction (PSD: position-sensitive x-ray detector). (*e*)–(g) Experimental arrangements (schematically) for measuring for grazing HCI–surface impact (*e*) initial charge-state-dependent outgoing projectile trajectories, (*f*) scattered projectile charge-state distributions, and (*g*) kinetic energy loss of scattered projectiles. (*h*) Measuring HCI-induced 'potential sputtering' of insulator films by means of a highly-sensitive quartz microbalance.

with a surface electron such that the latter becomes ejected and the former demoted, or another surface electron is captured into the projectile and the initially excited electron ejected. In contrast to AN, energy distributions of electrons from AD are directly related to the S-DOS.

Neutralization of HCI via multiple RN will be followed by autoionization (AI, see below and section 3) of the projectile near and at the surface. Energy distributions of slow electrons resulting from AI are no longer related to the target S-DOS.

Hagstrum (1954b) applied electronic transitions (a)–(d) in an adiabatic model (no coupling between electronic and nuclear motion) in order to derive the total slow electron yield. The respective transition rates increase exponentially with decreasing ion–surface distance according to the overlap between the S-DOS and the projectile-based electronic wavefunctions. Consequently, these transitions start most probably from the Fermi edge of the S-DOS. By assuming these transition probabilities as independent of the ion impact velocity, neutralization of a singly charged ion is found to take place most probably at distances of a few ängströms, whereas neutralization of a HCI, depending on its charge state $q$, can start at a comparably much larger distance (see section 3).

(e) *Autoionization* (AI) of a projectile was first found as Auger de-excitation of doubly excited projectiles following the impact of $He^{2+}$ or metastable $He^{+}$ (Hagstrum and Becker 1973). Arifov *et al* (1973) predicted that the neutralization of a HCI involves the transient formation of multiply-excited neutral projectiles which are subject to AI, thereby ejecting some of the excited electrons into vacuum and demoting the remaining ones to lower projectile states.

(f) *Quasi-resonant neutralization* (QRN) is a near-resonant electron transition between target and projectile core states, which can only take place in close collisions where a sufficient overlap of inner electronic orbitals is achieved. Such QRN is of interest in the later stage of HA relaxation at the target surface and in the bulk.

(g) *Radiative de-excitation* of excited projectile states after RN or AN of singly charged ions is much less probable than Auger de-excitation, since the respective transition rates will be about six orders of magnitude smaller than for Auger transitions. However, since radiative transition rates increase with about the fourth power of the projectile core charge (Bethe and Salpeter 1957), whereas Auger transition rates are not strongly affected by electron–core interaction, the latest steps in HA relaxation which involve the recombination of inner shell vacancies may also occur via soft x-ray emission (see below).

Careful experimental studies on slow HCI–surface interaction require sufficiently intense HCI beams. An important boost to this field has thus been given by novel powerful HCI sources such as the ECRIS (electron cyclotron resonance ion source, see review by Melin and Girard 1997), the EBIS (electron beam ion source, see review by Stšckli 1997) and the EBIT (electron beam ion trap, see Schneider *et al* 1991). In particular, ECRIS have been instrumental for first measurements of PE yields and energy distributions with higher charged ions than were available until about 1985. Such measurements have been performed for impact of up to $Ar^{12+}$ on both clean polycrystalline (Delaunay *et al* 1985, 1987a) and monocrystalline tungsten (de Zwart 1987). Until then, a linear dependence between the total PE yield and the potential energy carried by the HCI had been assumed to hold from the studies by Arifov *et al* (1973). However, Delaunay *et al* (1985) found beyond $Ar^{8+}$ a clear deviation from such a linear relationship (see also Delaunay *et al* 1987a), and de Zwart (1987) observed distinct peaks near 200 eV in the electron energy distributions which he ascribed to Ar inner shell (LMM, LMN, etc) Auger transitions (see also de Zwart *et al* 1989). At about the same time Zehner *et al* (1986) found projectile KLL Auger electron emission in studies on grazing incidence of $N^{6+}$ and $O^{7+}$ on clean monocrystalline gold, and Delaunay *et al* (1987b) observed similar results for impact of slow $N^{6+}$ and metastable $N^{5+}$ on polycrystalline tungsten. It was soon realized that such projectile inner shell transitions occur mainly in the later stage of HCI neutralization and thus after the bulk of slow electrons have been emitted by AI of the HA which is already formed in front of the target surface.

However, a relatively small fraction of the fast Auger electrons (typically less than 10%)

can be emitted before the projectile has touched the solid, as shown by Meyer *et al* (1991a, b), Das and Morgenstern (1993), Morgenstern and Das (1994) and Stolterfoht *et al* (1997) from studies involving high-resolution Auger electron spectroscopy (for a typical experimental arrangement, see figure 3(*b*)) and also by comparison of such measured electron spectra with modelled ones (Limburg *et al* 1995a, Stolterfoht *et al* 1995). Such measurements have been of great help towards an increasingly detailed understanding of the temporal sequence of HA decay.

Greater insight into the early stage of HA formation and decay in front of the surface resulted from measured slow electron multiplicity distributions (Lakits *et al* 1989, Kurz *et al* 1992, 1993a, b), which provided total PE yields as their mean values and also showed whether the respective slow electrons are mainly emitted still in front of and at the surface, or already from the target bulk (Aumayr and Winter 1994). Figure 3(*c*) sketches an experimental set-up for measuring electron-multiplicity distributions (for recent developments, see section 4).

Apart from emission of slow and fast electrons, the potential energy deposited into the HA can also be disposed of by soft x-ray emission, depending on the fluorescence yield for the respective projectile core. This was first demonstrated by Donets (1983, 1985) and then investigated in greater detail by means of high-resolution x-ray spectroscopy by Briand *et al* (1990). Figure 3(*d*) presents a typical experimental arrangement for such studies. More recent developments in this field may be found in Briand *et al* (1996) and Winecki *et al* (1996) and references therein.

A completely different access to HA properties is possible by studying the trajectories, charge state distributions and kinetic energy losses of projectiles for grazing HCI incidence on flat monocrystalline target surfaces (see figures 3(*e*)–(*g*)). De Zwart *et al* (1985) could demonstrate that projectile inner shell vacancies can survive close projectile collisions with surface atom cores, and Folkerts *et al* (1995) showed that final projectile charge state distributions from slow HCI channelling along a Au single crystal surface are practically independent of incident ion charge, which indicated that the ion charge equilibration occurs within only about 30 fs near the surface. Of special importance were studies of projectile trajectories in grazing incidence of HCI on clean, very flat monocrystalline surfaces, where specular reflection of ions with higher initial charge shows slightly steeper inclination of the outgoing trajectory. This could be assigned to stronger projectile image-charge attraction for higher initial $q$ along the incoming trajectory until the complete formation of a neutral HA (Winter 1992). It was especially interesting to perform such scattering experiments for insulator surfaces where the image-charge formation involves mechanisms different from those for metals.

Finally, we mention some experiments on HCI-induced sputtering and secondary ion emission from insulator surfaces, which are closely related to HA formation in front of such surfaces. No influence of projectile charge on sputtering yields is found for metallic (Neidhart *et al* 1995c) or semiconducting target surfaces (de Zwart *et al* 1986). This is to be expected as long as sputtering of neutrals (Sigmund 1993) and ions (Benninghoven *et al* 1994) is caused by the kinetic projectile energy (kinetic sputtering) only. However, for HCI impact on insulator surfaces a so-called 'Coulomb explosion' process has been predicted by Bitenskii *et al* (1979) and Bitensky and Parilis (1989), which is initiated by rapid extraction of a large number of electrons into the approaching HCI, resulting in highly localized positive surface charge-up and subsequent ablation of positively charged target ion cores. Such 'Coulomb explosion' was mainly pursued for HCI impact on alkali halide surfaces, for which 'electronic sputtering' and ion-induced desorption are well-established phenomena (Betz and Wien 1994, Varga and Diebold 1994). Total sputtering yields have been measured for MCI impact on polycrystalline LiF deposited on the face of a quartz microbalance crystal (see figure 3(*h*), after Neidhart *et al*

1995a). Such measurements showed no impact energy threshold and a dramatic increase of the total sputtering yield with ion charge, both are in striking contrast to kinetic sputtering. The mechanism thus responsible has been termed 'potential sputtering' because it could not be reconciled with the above-mentioned 'Coulomb explosion' process (see further discussion in section 4). We remark that HCI-induced secondary ion yields from clean LiF (Neidhart *et al* 1995b) are typically by a factor of a hundred smaller than the total sputter yields, which shows that the dependence of the secondary ion yield on the projectile charge $q$ cannot provide sufficient information on the here-presented potential sputtering process.

Summing up, the following signatures constitute principal experimental evidence for HA formation and decay in the course of slow HCI–surface interaction.

(a) Slow HCI will already be completely neutralized before they touch a clean metal surface. This is seen from the projectile scattering trajectory which is subject to image-charge attraction until the latter disappears upon formation of the neutral HA, which can be shown to occur well before close surface contact. Another proof of complete HA neutralization in front of the surface is the saturation of the total slow electron yield towards nominal-zero HCI impact energy. Furthermore, the image-charge attraction sets an effective minimum impact energy for slow HCI approaching a metal surface. For insulator surfaces this situation is considerably more complex, as will be discussed in sections 3 and 4.

(b) The number of emitted slow electrons as measured by different methods is much larger than the respective HCI charge. This fact and the respective electron multiplicity distributions demonstrate a rapid AI of the HA which will be re-fed by ongoing RN to keep it in a fully neutralized state.

(c) Fast Auger electrons and soft x-rays resulting from projectile inner shell de-excitation provide complementary and mutually compatible information mainly on the late stage of HA relaxation. By studying such processes for different impact velocities and angles in comparison with modelling calculations, further details on the time sequence of HA relaxation can be obtained.

(d) Potential sputtering induced by impact of HCI on particular insulator surfaces is a recently observed process which can be explained by defect-mediated desorption, in full agreement with the other signatures for HA formation and decay.

## 3. Theory of HA formation and decay

Neutralization of a HCI in front of a solid surface involves genuine multi-electron capture of dozens up to several hundreds of electrons and a complex many-body response of the solid due to its strong perturbation by the projectile. In the following we will briefly review the historic development of the theoretical description of these processes and then present our currently assumed scenario for the interaction of a slow HCI with an atomically clean metal surface. Practically the same scenario can be adopted for HCI impact on semiconductor surfaces, whereas some important differences in the response of metal and insulator surfaces will be pointed out whenever appropriate.

As already explained in section 2, the first attempts to model the interaction of slow singly, doubly and multiply charged ions with a metal surface was made by Hagstrum (1954b), who described this interaction by stepwise electronic transitions. His 'adiabatic quantum model' was further developed by Arifov *et al* (1973). In their view the ion–solid interaction started by multiple electron capture into high $n$-states as resonant 'tunnelling' through the potential barrier and produces a multiply-excited particle. Due to the efficient overlap of close lying $n$-levels the resulting autoionization decay proceeds in a so-called 'ladder sequence' and gives

rise to the emission of slow electrons. In this way the initial potential energy of the approaching projectile is dissipated in many small steps—a linear relation between the potential energy of the primary ion and the yield of emitted slow electrons was predicted and also observed, see Arifov *et al* (1973). However, this linear relation has to break down if later steps of the ladder involve more energetic transitions (Delaunay *et al* 1985, 1987a), in particular within inner shells (Zehner *et al* 1986, de Zwart 1987). In addition, the ladder model faces the principal difficulty of the so-called 'bottleneck problem' (Burgdörfer 1993). From a simple estimate of the distance where the projectile starts to interact with the surface, Delaunay *et al* (1987a) found that the time available for complete relaxation of a projectile to its neutral ground state would have to be less than $10^{-13}$ s if this relaxation is to be completed still in front of the surface. Since, on the other hand, typical AI rates are usually not larger than $10^{14}$ $s^{-1}$ and a number of steps are necessary to complete the whole ladder sequence, the projectile will hit the surface long before its AI relaxation has been completed.

Proposals to circumvent this bottleneck problem (Andrä 1988, 1989, Vaeck and Hansen 1995) by, e.g., assuming anomalously high Auger rates were unsuccessful in explaining the then-available experimental findings. Somewhat more refined theoretical treatments by Apell (1987) and Snowdon *et al* (1988) assumed larger distances for the first electron capture, and a classical field emission approach was presented by Bardsley and Penetrante (1991). The breakthrough finally came with the COB model, which was originally developed for one-electron capture in HCI–atom collisions by Ryufuku *et al* (1980) and later extended to multiple electron capture by Barany *et al* (1985) and Niehaus (1986). Based on the treatment for ion–surface collisions (Burgdörfer *et al* 1987), these COB models were adapted to HCI–surface impact (Burgdörfer *et al* 1991, Burgdörfer 1993, Burgdörfer and Meyer 1993, Lemell *et al* 1996). In the following we will briefly review key elements of a now widely accepted scenario for HCI–surface interaction, which is largely based on the above COB model and involves at least the following two stages (see figure 2).

(I) The approach of the projectile towards the surface up to close contact.
(II) Relaxation of the projectile to its ground state within the target bulk (alternatively, backscattering of the projectile into vacuum).

In both stages the target material plays an important role which can be easily understood if we compare metallic and insulating targets (figure 4). Whereas in metals the conduction band is divided by the Fermi level into occupied and unoccupied regions and work functions are typically 4–6 eV, in insulators the least-bound electrons form a completely occupied valence band with comparably larger binding energy (typically 6–12 eV), which is separated by a band gap (forbidden states) of several eV width from the first allowed states in the completely empty conduction band. In addition, the dielectric response of an insulator, which is governed by a frequency-dependent dielectric function $\varepsilon(\omega)$, is quite different from the one for metals.

Let us describe the sequence of HA formation and decay for a metal target for the approach of a slow HCI (charge state $q$; projectile velocity $v_p \ll v_F$, with $v_F$ the Fermi velocity of electrons in the metal target) towards a metal surface (usually characterized in the jellium approximation by a conduction band with the work function $W_\phi$ and Fermi energy $E_F$, see figure 4).

The HCI–surface interaction causes a collective response of the metal electrons which can be approximated at large distances by the classical image potential. The latter accelerates the HCI towards the metal surface and therefore sets a lower limit to the effective projectile impact velocity, which corresponds to an upper limit for the available HCI–surface interaction time. In addition, the image interaction shifts the weakly bound projectile electron states and decreases the height of the electronic potential barrier between the HCI and the surface which

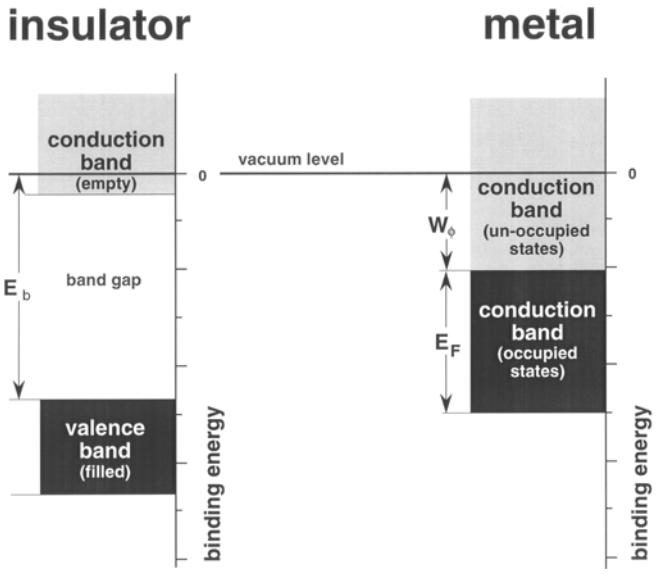


**Figure 4.** Occupied, unoccupied and forbidden electron states in a typical insulator as compared with a typical metal.

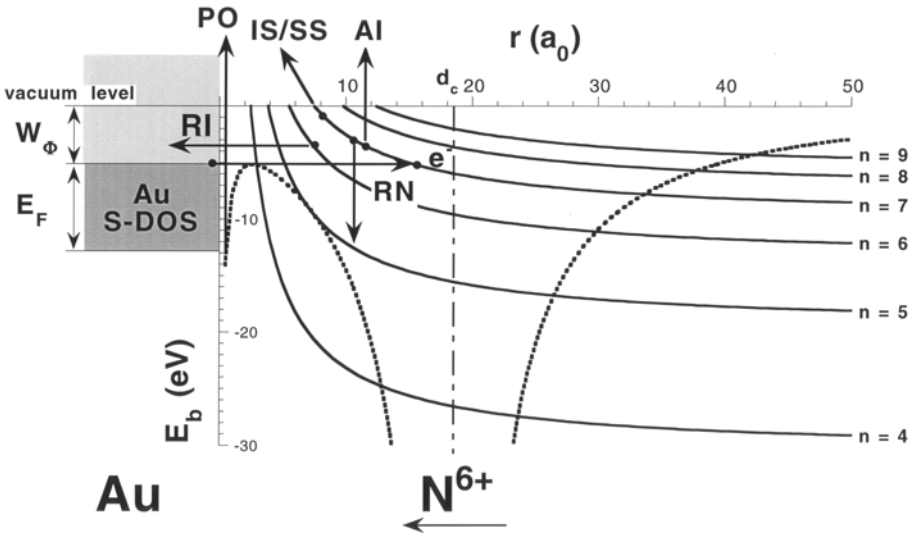


**Figure 5.** Potential barrier between a metal surface (Au) and a HCI ($N^{6+}$) at a distance from the surface of about 18 au. The potential barrier between the ion and the surface has already decreased below the Fermi level of Au and electron capture (RN) becomes classically allowed (see text).

is formed by the potential of the projectile, its image potential and the image potential of the electron to be captured (see figure 5). At a critical distance (atomic units are used unless otherwise stated)

$$d_c(q) \approx \sqrt{2q}/W_\phi \tag{1}$$

the potential barrier between the metal and the projectile drops below the Fermi level and

electrons from near the Fermi edge of the metal surface can be transferred to the incident projectile (see figure 5). In general, resonant COB transitions (RN, see section 2) will be favoured and thus highly excited states of the projectile will be populated. In principle RN is already possible at somewhat larger distances via tunnelling through the potential barrier, but this has been found of minor importance (Burgdörfer *et al* 1991, Burgdörfer 1993). The COB model also predicts the principal quantum number $n_c$ of the highly excited projectile states into which the first RN transitions will take place:

$$n_c \approx \frac{q}{\sqrt{2W_\phi}} \frac{1}{\sqrt{1+\frac{q-0.5}{\sqrt{8q}}}}. \tag{2}$$

With its further approach the projectile levels become shifted upwards (see figure 5) in energy due to image interaction (IS) and screening of the projectile charge by the already captured electrons (SS). Now, also, somewhat lower projectile $n$-shells can be populated either by cascading from AI transitions or because these levels now fall into resonance with states at the Fermi edge. On the other hand, previously populated higher levels can be emptied by RI into the conduction band, AI and promotion above the vacuum level (figure 5). This interplay of electronic transitions goes on during the projectile's approach towards the surface and will gradually move the population to lower $n$-levels (Burgdörfer *et al* 1991, Andrä *et al* 1991).

Projectile states will be populated and again emptied within just a few femtoseconds and can therefore not be considered as stationary states, as was pointed out by Burgdörfer (1993).

Slow electrons can be emitted from the projectile, mainly via AI and to a lesser extent also via IS/SS promotion into vacuum, but they will be rapidly replaced by RN and therefore the projectile becomes and remains completely neutralized above the surface, with its electrons distributed among a number of highly excited levels. In this way the HA, which is of highly transient nature, will be formed. The projectile is subject to image-charge acceleration until its complete neutralization. Its corresponding kinetic energy gain $\Delta E_{q,im}$ is closely related to the distance of neutralization as predicted by the COB model (equation (1)). If one considers stepwise neutralization at the $q$-related over-barrier distance given by equation (1) ('staircase approximation'), the energy gain for a HCI with charge state $q$ at a metal surface with work function $W_\phi$ becomes (Burgdörfer *et al* 1991, Burgdörfer 1993)

$$\Delta E_{q,im} \approx \frac{1}{3\sqrt{2}} W_\phi q^{3/2}. \tag{3}$$

About three-quarters of this value will already have been gained by the projectile on its way from far away to the distance $d_c$ of the very first RN transition (the so-called 'classical lower limit'). Measurements of $\Delta E_{q,im}$ with different experimental techniques are in very satisfactory agreement with the COB model (see section 4 and Winter 1992, Aumayr *et al* 1993, Winter *et al* 1993, Aumayr and Winter 1994, Kurz *et al* 1994, Lemell *et al* 1996). Figure 6 demonstrates the formation and decay of a HA as calculated from the COB model for a slow $Pb^{40+}$ ion approaching a Au surface according to Lemell *et al* (1996). The dot in the projectile centre represents its core with the occupied inner shells ($n = 1$–4), and $R$ is the distance between the projectile and the surface. The first RN which occurs at $R = d_c \approx 45$ au will, according to equation (2), populate highly excited states of the projectile ($n \approx 35$ for $Pb^{40+}$ on Au). Since quasi-neutrality is reached very rapidly (see figure 7) and the mean radius $\langle r \rangle_n$ of the most probably populated shell (darkest contour in figure 6) is of the order of the ion–surface distance, the term HA is quite appropriate for this intermediate compound. As $R$ decreases, the size of the charge cloud will shrink accordingly.

However, this process cannot occur instantaneously since depopulation of the outer shells proceeds with a finite loss rate involving AI and reionization into unoccupied states of the

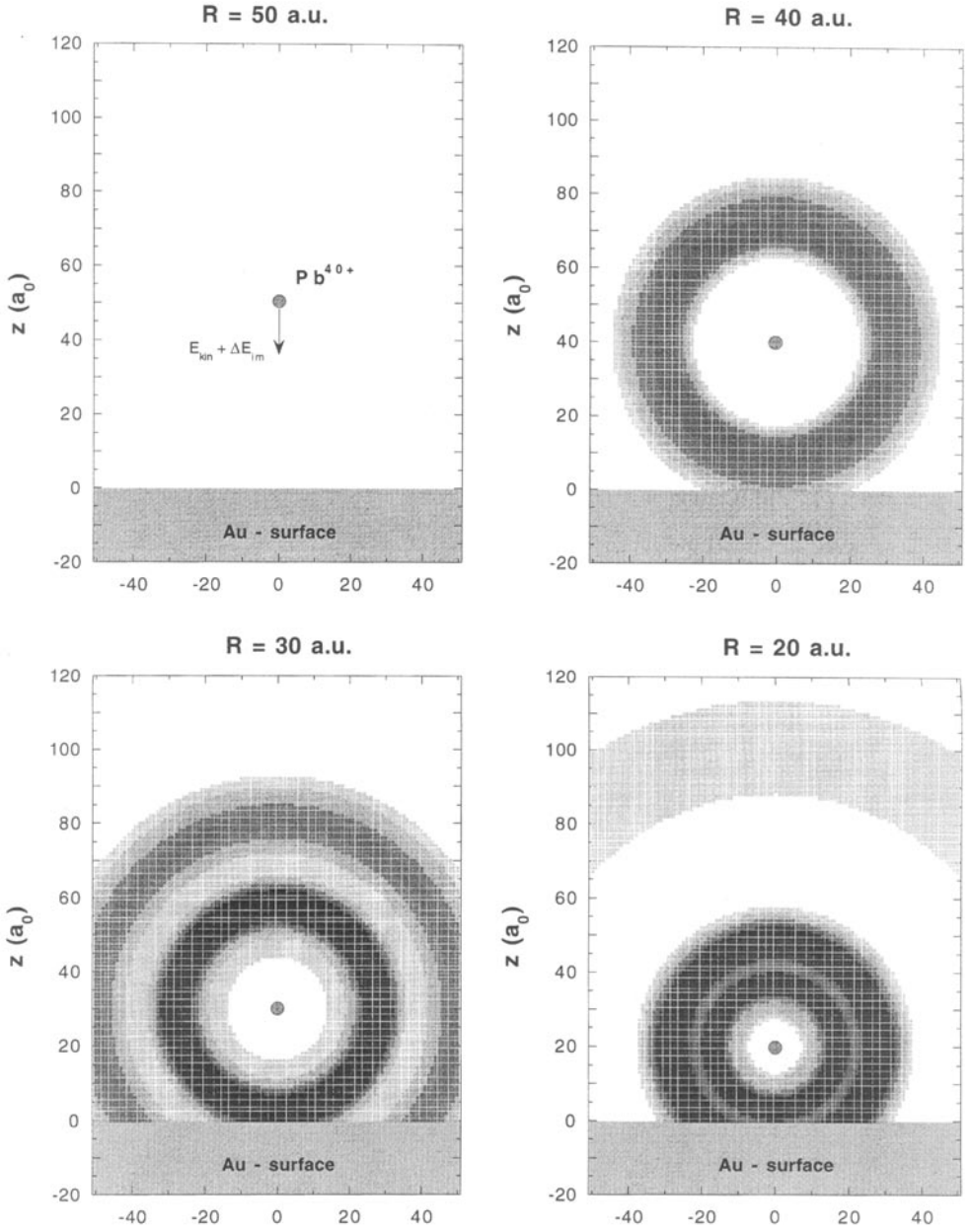


**Figure 6.** Evolution of a hollow Pb atom with initial charge state of $q = 40$ according to a COB simulation by Lemell *et al* (1996).

solid or into the continuum. Image charge attraction further limits the available ion–surface interaction time until projectile impact, and therefore relaxation of the HA to its neutral ground state via electronic interactions is usually far from complete when the projectile enters a region of sizeable surface electron density (the so-called selvedge). Here the metal electrons form a dynamic screening cloud around the ionic projectile core, which gradually 'peels off' (PO)

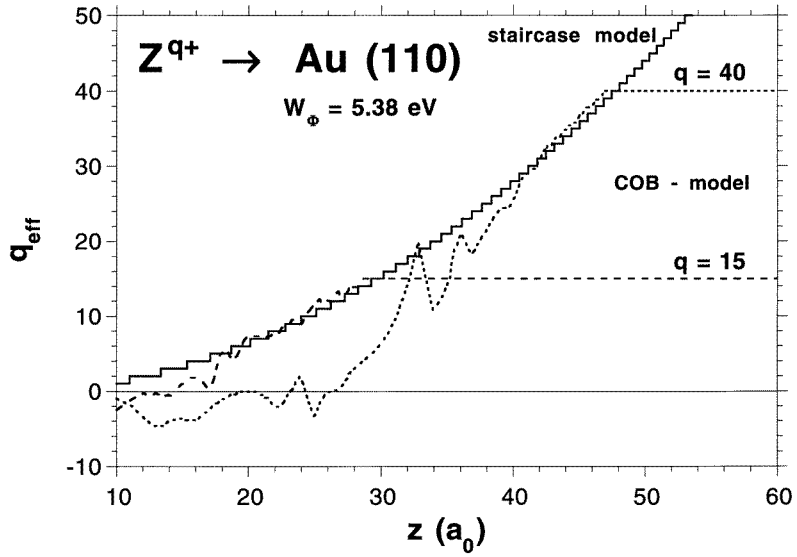


**Figure 7.** Evolution of the effective charge state $q_{eff}$ for a projectile in initial charge states $q = 40$ and $q = 15$, respectively, as calculated according to the COB model (Lemell *et al* 1996). Also shown is the charge-state evolution according to the staircase model (equation (1)).

(Burgdörfer 1993, Kurz *et al* 1993a, b, Aumayr and Winter 1994) those electrons which have earlier been captured into outer projectile states. At the bulk electron density all projectile electrons with larger Rydberg radii than the screening distance $v_F/\omega_p$ ($\omega_p$ is the plasmon frequency) are removed from the projectile and effectively replaced by a dynamic screening cloud of metal conduction band electrons (Arnau *et al* 1995, Stolterfoht *et al* 1997).

During the above-described interaction further slow electrons will be emitted from the HA, but only some of them will be able to escape into vacuum and thus to contribute to the total electron yield. Escape fractions for electrons released near the surface via AI and PO have been calculated by Lemell *et al* (1995). Screening of the projectile in the first few layers of the surface by conduction band electrons produces a new kind of HA ('HA of the second generation'), with its relaxation determined by two competing processes. At low projectile velocity Auger transitions from the electron screening cloud fill remaining L- or M-shell holes of the projectile (Diez Muino *et al* 1996), but at higher impact velocity quasi-resonant vacancy transfer can take place in close collisions between HA and target core states by level crossing of the Landau–Zener type and orbital promotion (Fano and Lichten 1965, Burgdörfer *et al* 1995, Stolterfoht *et al* 1995). Filling of the inner shell vacancies (including K-shell holes) will terminate the relaxation of the projectile (Diez Muino *et al* 1998) by giving rise to the majority of observable fast Auger electrons. During this last step, x-ray emission can become competitive to Auger electron emission (Briand *et al* 1990) and therefore deliver information on such HA of the second generation. In addition, the dissipation of an important fraction of the potential energy originally carried by the HCI can also cause the removal of atoms and ions from the target ('potential sputtering', see section 4).

If the kinetic energy of the projectile is sufficiently high to cause kinetic electron emission (KE), this can contribute to the slow electron yield (Lakits *et al* 1990, Hasselkamp 1992, Varga and Winter 1992, Eder *et al* 1999). A projectile may also eventually become back-scattered from some point on its trajectory at or below the surface. For grazingly incident HCI, this

back-scattering can take place as specular reflection of the projectile at the repulsive planar surface potential (Winter 1992), in which case the further projectile de-excitation will proceed on the outgoing trajectory (Burgdörfer *et al* 1995). The exit angle, charge states and energy loss of such specularly scattered projectiles also provide insight into HA dynamics (see section 4).

Most of the theoretical work so far has dealt with HA formation above perfectly conducting targets (i.e. metals). Insulating targets differ from conducting ones primarily by their electronic structure (see figure 4) and dielectric response to rapidly varying external electric fields, which can be characterized by a frequency-dependent dielectric response function $\varepsilon(\omega)$. The image-charge potential used in any theoretical approach will have to be modified by using $\varepsilon(\omega)$ (for a detailed description, see Arnau *et al* 1997). Barany and Setterlind (1995) were the first to generalize the COB model to insulating surfaces by using a simple finite dielectric constant $\varepsilon$ in the derivation of $d_c(q)$ and $\Delta E_{q,im}$ in equations (1)–(3). A more detailed COB model for HCI impact on ionic crystals (like LiF) was recently presented by Hägg *et al* (1997, 1998). This model not only included the frequency dependence of $\varepsilon(\omega)$ in the calculation of the image potential, but also considered the Madelung and polarization potentials in describing the electronic potential governing electronic transitions between the ionic crystal and the HCI. The model could successfully explain a weak dependence of the energy gain by image-charge attraction on the parallel projectile velocity component, as has been observed in experiments for grazing incidence of HCI on LiF (Yan and Meyer 1997). Other difficulties associated with insulating surfaces arise because HA formation strongly depends on the history of the previous neutralization sequence, i.e. from which sites previous capture events have taken place.

## 4. Selected experimental results and discussion

Considering the large number of studies which have been devoted in recent years to the subject of this review, we will discuss here only a few recent developments in which the present authors have been directly involved. For a fairly complete account on the subject up to 1997 the reader is referred to the review of Arnau *et al* (1997).

### *4.1. Image charge acceleration and timescale for HA formation and relaxation*

Formation of HA is associated with neutralization processes which gradually switch off the image charge force acting on the projectile in front of the surface. Therefore the kinetic energy which a HCI gains due to image charge acceleration will be directly related to the distance $r_c$ of its first complete neutralization according to equation (1). Winter *et al* (1993) first derived this energy gain from the increased scattering angles of grazingly incident $Xe^{q+}$ as compared with equally fast neutral Xe projectiles (for their method see section 2). These measurements were made with very flat Al(111) and Fe(110) target surfaces, and similar work has been performed for HCI of Pb scattered on Au(110) by Meyer *et al* (1995).

In a different in principle experimental approach Aumayr *et al* (1993) and Kurz *et al* (1994) deduced the energy gain due to image charge acceleration from the impact-velocity dependence of the total electron yield for normal impact of HCI (charge states up to $q = 79$) on polycrystalline Au. This method makes use of the fact that the average number of emitted slow electrons depends on the time interval between the first RN and 'touch-down' of the projectiles on the surface (see figure 8 and section 2). Their data and the results of Meyer *et al* (1995) are plotted in figure 9 as a function of the initial charge state $q$ and compared with predictions of the COB model. All experimental data exceed the classical lower limit which assumes instantaneous neutralization at the critical distance $r_c$ for first RN (see section 3), but closely follow the staircase approximation according to equation (3) of the COB model which

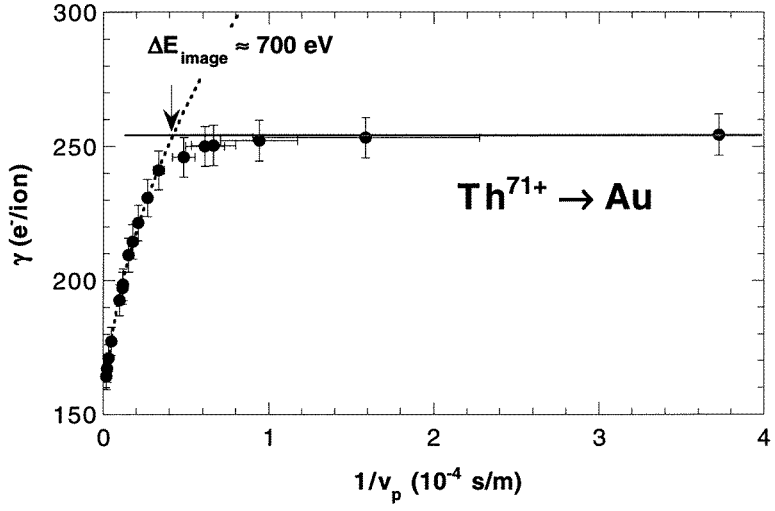


**Figure 8.** Measured total electron yield $\gamma$ versus inverse nominal projectile velocity $v_p^{-1}$ for impact of $Th^{71+}$ on clean polycrystalline Au (Aumayr *et al* 1993).

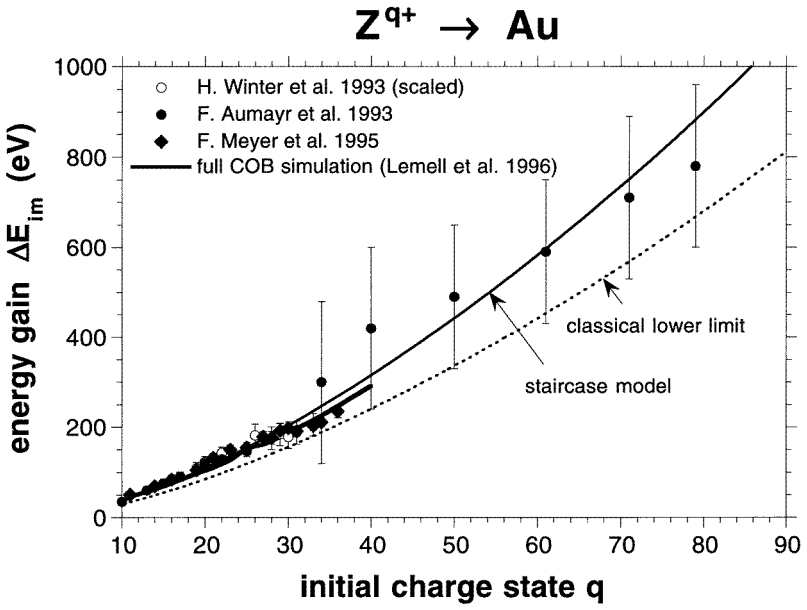


**Figure 9.** Energy gain due to image acceleration. Experimental data (symbols) are compared with a full COB simulation (Lemell *et al* 1996) as well as with the staircase limit (equation (3)) and the classical lower limit (i.e. instantaneous neutralization at $d_c$).

involves stepwise neutralization. Even fine details (e.g. a small deviation around $q = 30$) have recently been explained by Lemell *et al* (1996). When using a full COB simulation code instead of the staircase approximation the calculated energy gain due to image charge acceleration also decreases below the staircase value (equation (3)) for projectile charge state $q > 20$, but still exceeds the instantaneous neutralization case. This behaviour is due to the fact

that for high $q$ the HA which is formed upon approach toward the surface can accommodate a larger number of electrons than $q$ because of incomplete Slater screening of the projectile core (Lemell *et al* 1996). Being thus in agreement with all available data sets, this full COB model can be regarded as a good description of the neutralization of a HCI in front of a metal surface.

The image charge attraction causes a minimum impact velocity and therefore limits the available ion–surface interaction time, i.e. the time between first RN and 'touch down' on the surface, to less than 50 fs. Since characteristic Auger rates are far too slow to allow for a complete relaxation of the HA to its ground state before this 'touch-down' (the bottleneck problem: Burgdörfer 1993, Burgdörfer *et al* 1995), measurements of the time needed for total relaxation yield important information on processes occurring after close contact with the surface. A good estimate of the total relaxation time has been derived by Folkerts *et al* (1995) from final projectile charge state distributions for scattering of $O^{q+}$ at small angles of incidence (surface channelling) from a Au(110) surface. The experimental conditions were chosen such that the projectiles spent less than 30 fs within 2 Å of the topmost Au surface layer, and less than 60 fs in the region where electron transfer is in principle possible. These authors observed that in spite of this very short time, the projectiles reach a stationary charge state distribution which practically does not depend on the primary ion charge state $q$. This implies that within typically 30 fs vicinity of the surface a complete relaxation of the electronic projectile states has taken place. In an extended COB simulation Burgdörfer *et al* (1995) could show that quasi-resonant capture (QRN) into the L-shell of the projectile proceeds sufficiently fast to explain the observed total relaxation time.

### *4.2. Low-energy electron yields and number statistics of electron emission*

The HA relaxation is associated with emission of a large number of electrons via AI, AN, PO, etc (see section 3). Total slow electron yields and slow electron number statistics therefore contain information on this phase of the HA history. In early measurements (Hagstrum 1954a, b, Arifov *et al* 1973) a linear dependence of the total electron yield on the projectiles' potential energy (i.e. the sum of the $q$ first ionization potentials) has been found.

This indicated a multi-step RN/AI relaxation cascade in front of the surface. Although this linear relationship between the total electron yield and potential energy breaks down above a certain charge state (Delaunay *et al* 1985, 1987a, de Zwart 1987, see section 2), no saturation of the total electron yield as a function of charge state could be observed even for very high charge states (Aumayr *et al* 1993, Kurz *et al* 1994). Typical sets of absolute total electron yields which have been obtained from electron multiplicity measurements for impact of slow HCI up to $q = 80$ are shown in figure 10. These total electron yields exhibit the following general dependence on impact velocity. Starting at low collision velocity the electron yield drops continuously towards a minimum value and then rises again due to additional kinetic electron emission (KE, see figure 11). KE starts for clean Au at a threshold impact velocity of about $2 \times 10^5$ m s$^{-1}$ (Lakits *et al* 1990) and provides an electron yield which first rises about linearly with impact velocity. For the total electron yield $\gamma$ in the exclusive PE regime (i.e. below the onset of KE) the following empirical relation was found (Kurz *et al* 1992, 1993a, b, Vana *et al* 1995a)

$$\gamma_{PE}(v) = \frac{c}{\sqrt{v}} + \gamma_\infty \tag{4}$$

where $c$ and $\gamma_\infty$ are constants depending on the collision systems under consideration. Of course the velocity $v$ should be taken as the effective projectile velocity, i.e. including the respective image-charge acceleration. In order to extract information on the above-surface

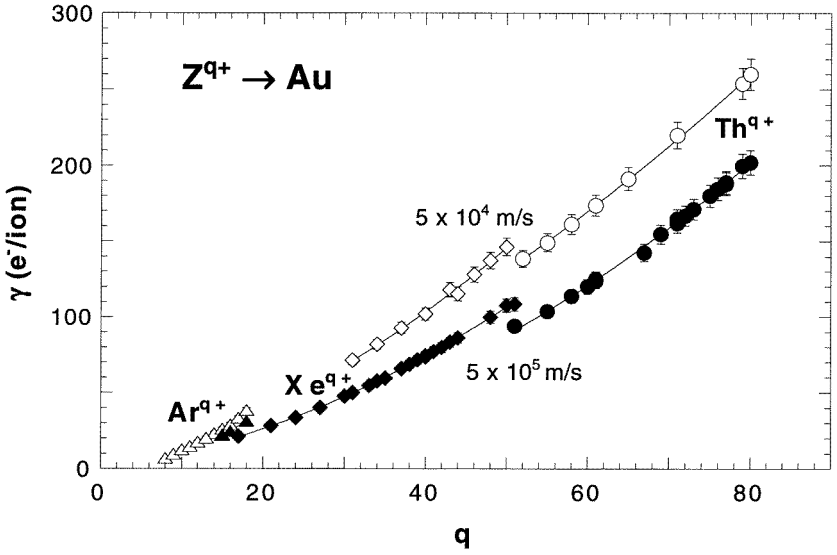


**Figure 10.** Charge state dependence of electron emission yields for HCI hitting a clean Au surface, for two different impact velocities (Kurz *et al* 1994).

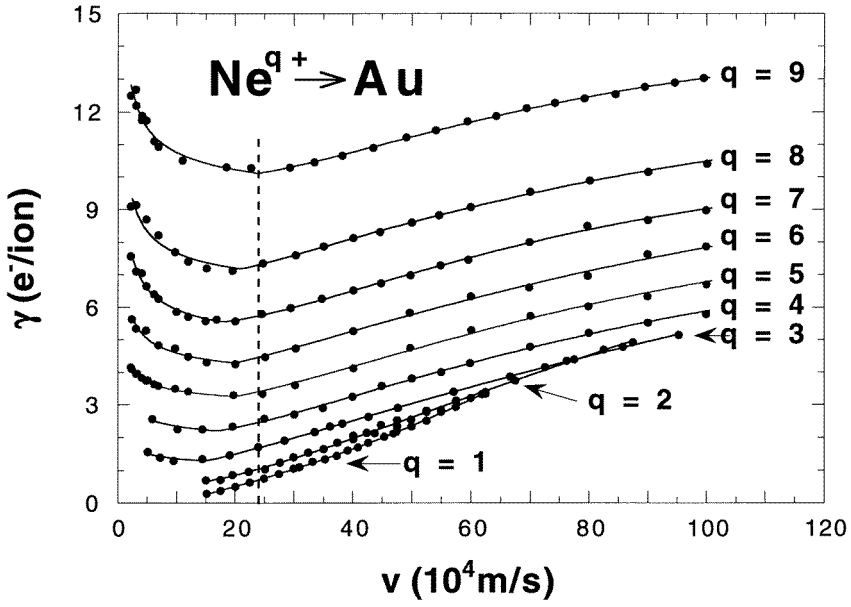


**Figure 11.** Total electron yields versus impact velocity as derived from the measured ES, for impact of $Ne^{q+}$ ions on a clean Au surface (Eder *et al* 1999).

neutralization steps of the HCI, these measured total electron yields have been compared with elaborate COB model calculations (Kurz *et al* 1993a, b). Qualitatively, increase of the electron yield towards low collision velocity (see figures 8 and 11) as described by the first term in equation (4) is attributed mainly to Auger (AI) cascades which can produce the more electrons the more time is available in front of the surface. The velocity-independent part of the PE yield

denoted by the constant $\gamma_\infty$ in equation (4) is mainly attributed to fast PE processes already arising close to the surface (electron promotion, screening, PO, etc). Actually, close to the surface we can no longer distinguish between electrons in the conduction band and those on the projectile, since the latter core will be 'dressed' by conduction band electrons.

Consequently, atomic Auger transition rates should be about as fast as the Auger neutralization rates (Diez Muino *et al* 1995, 1996, 1998).

Further insight into the origin of emitted PE electrons is provided by comparing the measured electron multiplicity distributions (ES) with model probability distributions (Vana *et al* 1995b, Winter *et al* 1996). In the first place, the assumption is made that these electrons are emitted independently from each other and with equal single emission probabilities. In this case the probability for emission of $n$ electrons will be given by the binomial distribution which contains the electron ensemble size, $N$, as a parameter. Thus, by fitting a binomial distribution to the measured ES, the single emission probability $p$ and the number $N$ of electrons which are actually involved in the HCI–surface interaction eventually causing the PE can be determined. ES measured at low HCI impact energy for both metal and insulator targets closely follow binomial distributions (Vana *et al* 1995b, Winter *et al* 1996), which can be taken as an indication that most of these electrons are ejected above and at the surface. On the other hand, electron emission arising mainly from below the surface, e.g. because of KE, shows ES which clearly deviate from the binomial distribution (Eder *et al* 1997).

### *4.3. Fast Auger electron and x-ray emission*

Recombination of inner shell vacancies accompanied by emission of fast Auger electrons or soft x-rays takes place mainly in the late stage in the HA relaxation cascade. High-energy Auger electron spectra show profound structures which, by means of Hartree–Fock atomic structure calculations, can serve for identifying the HA configuration at the moment of the Auger decay (Limburg *et al* 1994, Schippers *et al* 1994). Whether this emission occurs very close to, but still above, the surface or already below it was one of the most controversially discussed issues in this field (the interested reader is referred to, e.g., Meyer *et al* 1991a, b, Das and Morgenstern 1993, Köhrbrück *et al* 1994, Arnau *et al* 1997). The fact that most of the early measurements were made for comparably high projectile impact velocity with almost all fast Auger electrons coming from below the surface is only part of this problem.

From careful KLL Auger electron spectroscopy with slow $N^{6+}$ scattered at the first layer of a Au(110) target, Thomaschewski *et al* (1998) could show that a significant acceleration of the L-shell filling occurs already when the projectile passes through the region of increased electron density around the jellium edge (i.e. still above the first layer), and that under these conditions the KLL spectra remain almost independent of the amount of surface penetration.

In figure 12 we compare high-resolution KLL Auger spectra obtained for $N^{6+}$ ion impact on different target surfaces (Limburg *et al* 1995b). While results for semiconducting p-doped Si(100) are very similar to those for Al(110), a pronounced difference for the insulating LiF(100) was attributed to two competing filling mechanisms of the projectile L shell. The absence of the peak on the low-energy side of the KLL spectrum for LiF as compared with Si and Al (see figure 12), which corresponds to slow L-shell filling via Auger cascades, has been ascribed by Limburg *et al* (1995b) to insufficiently mobile electrons in LiF. For the LiF surface, the L-shell filling probably only starts after the projectile has entered the close collision region. By comparing results for $O^{7+}$-induced KLL Auger electron emission for a clean LiF surface and a Au target surface covered by up to a single monolayer of LiF, Khemliche *et al* (1998) have recently argued that it is not the large band gap, which only in the case of bulk LiF would restrain RI back into the target, but rather the high work function that hampers the

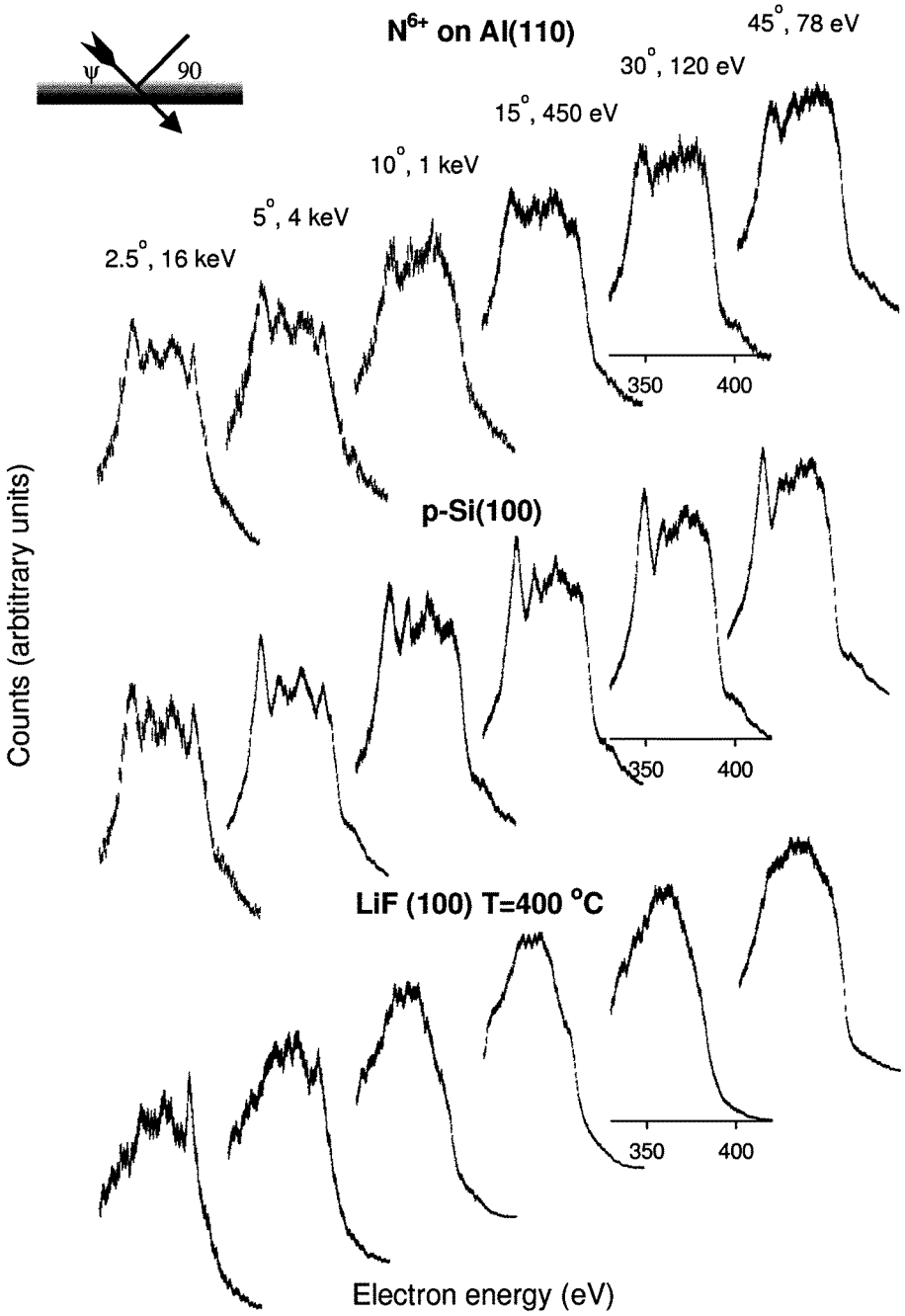


**Figure 12.** KLL Auger spectra of $N^{6+}$ on Al(110) (top), Si(100) (middle) and LiF(100) (bottom). Ion energy and incident angle have been varied in order to keep the ion velocity component normal to the surface constant. The ordinate is linear (Limburg *et al* 1996).

neutralization of HCI in front of insulating surfaces.

As already mentioned, recombination of inner shell vacancies can also proceed by

characteristic x-ray emission. From highly resolved x-ray spectra produced in HCI–surface collisions, the number of spectator electrons residing in higher $n$-shells at the moment of the radiative inner shell transition and the time scale for such inner shell filling in an HA can be estimated. Such measurements give direct evidence for the existence of HA (Briand *et al* 1990). However, as with the corresponding Auger electron spectroscopy, the question as to what extent the x-ray emission occurs still 'above' the surface or already 'inside' the bulk is not yet fully settled (Briand *et al* 1996, Aumayr *et al* 1997), whereas the x-ray spectra first reported by Briand *et al* (1990) are now unambigously attributed to arise from a 'HA of the second generation', i.e. from below the surface (see section 3).

### *4.4. Coincidence studies*

By using coincidence techniques Lemell *et al* (1998) could correlate electrons emitted from grazing incidence HCI scattering at a clean monocrystalline Au surface with specific projectile trajectories as characterized by their scattering angle. A clear separation of above- and below-surface HA de-excitation could be achieved in this way. Figure 13(*a*) shows the intensity distribution of scattered projectiles as recorded on a position sensitive detector for 0.45 keV amu$^{-1}$ $Ar^{8+}$ ions impinging with an incidence angle of 5° onto a clean flat Au(111) surface. The needle-like feature on the right-hand side of figure 13(*a*) is due to a small fraction of the primary ion beam that has passed above the target edge, while the broad peak represents the actually scattered projectiles. Particles scattered at the collective planar potential ('surface channelling': Winter 1992) of an ideally flat surface are specularly reflected and contribute only to the central peak of the angular distribution, while scattering from surface imperfections (e.g. steps) or subsurface channelling make their marks in the wings of the scattering distribution. As shown in figure 13(*b*), specularly scattered projectiles give rise to much less electron emission than projectiles emerging with larger scattering angles, i.e. on the wings of the scattering distribution. Corresponding electron multiplicity distributions (ES) are shown in figure 14(*a*) (ES taken in coincidence with the central part of the reflected particle distribution were labelled ①, those associated with the peripheral part by ②). Figure 14(*b*) shows an ES spectrum for $Ar^{8+}$ impact under normal incidence with a much lower total kinetic energy such that it has an equal velocity component normal to the surface as the specularly reflected particles. Clearly, the normal-incidence- and the grazing-incidence-related ES are practically identical around their maxima. These parts of the ES can therefore be unambiguously correlated to PE due to projectiles which are not penetrating the surface and thus approach the topmost surface layer not closer than about 1 au. An immediate consequence of this observation is that the above-surface PE part from HA relaxation is only governed by the perpendicular impact velocity component and does not depend on the parallel velocity.

### *4.5. Potential sputtering*

The extent to which the electronic relaxation of HA takes place above or below the surface is closely related to the way a HA dissipates its large potential energy. Emission of electrons and x-ray photons carries away only a fraction of the total potential energy originally stored in a HCI. The remaining part will be deposited into the solid and converted into electronic excitation of a small surface region (creation of electron–hole pairs, 'hot holes' in the conduction or valence band of the target and inner shell vacancies in target atoms). This electronic excitation may lead to important applications for material modification by means of slow HCI impact (e.g., novel cleaning procedures in the semiconductor industry, the nanostructuring of insulators). For metal surfaces, even rather sudden perturbations of the electronic structure

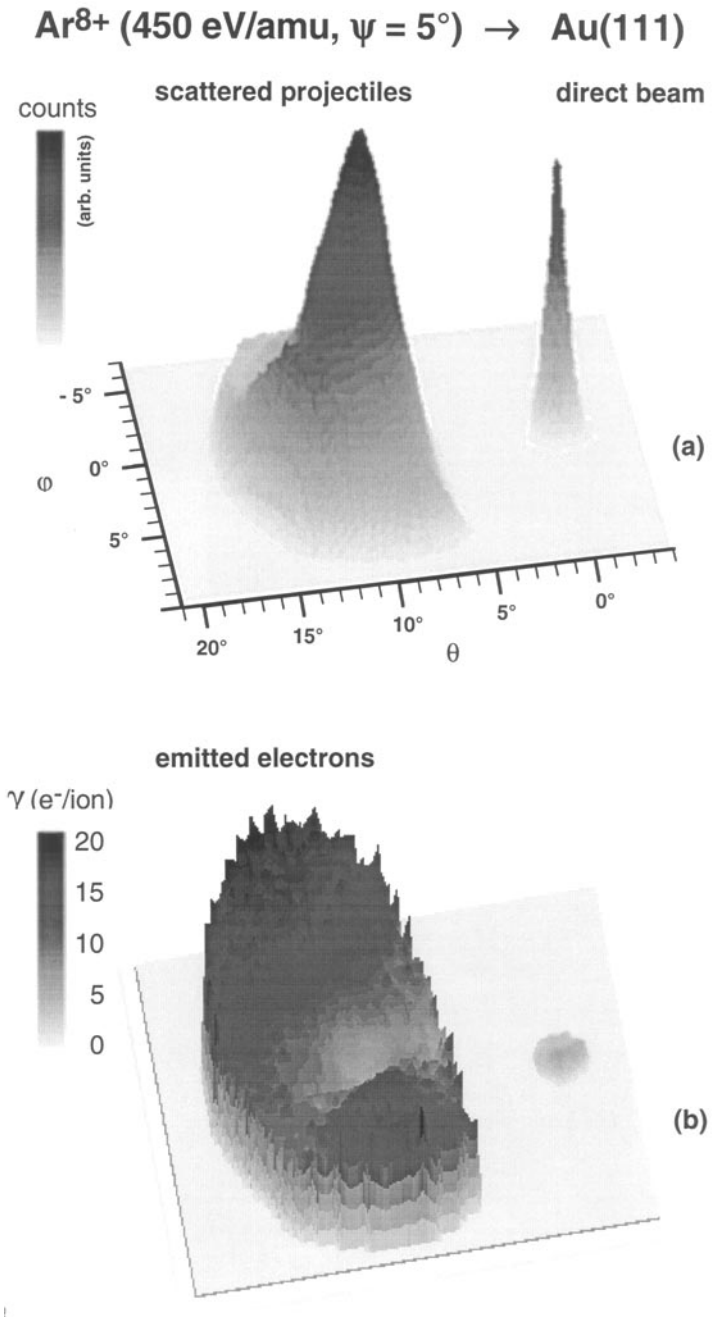


**Figure 13.** (*a*) Intensity distribution of scattered projectiles as recorded on a position-sensitive detector for the case of 0.45 keV amu$^{-1}$ $Ar^{8+}$ ions impinging under a grazing angle of 5° onto a Au(111) single crystal surface. (*b*) Mean number of emitted electrons measured in coincidence with projectile scattering under various exit angles (positions correspond to figure 13(*a*)). (Lemell *et al* 1998.)

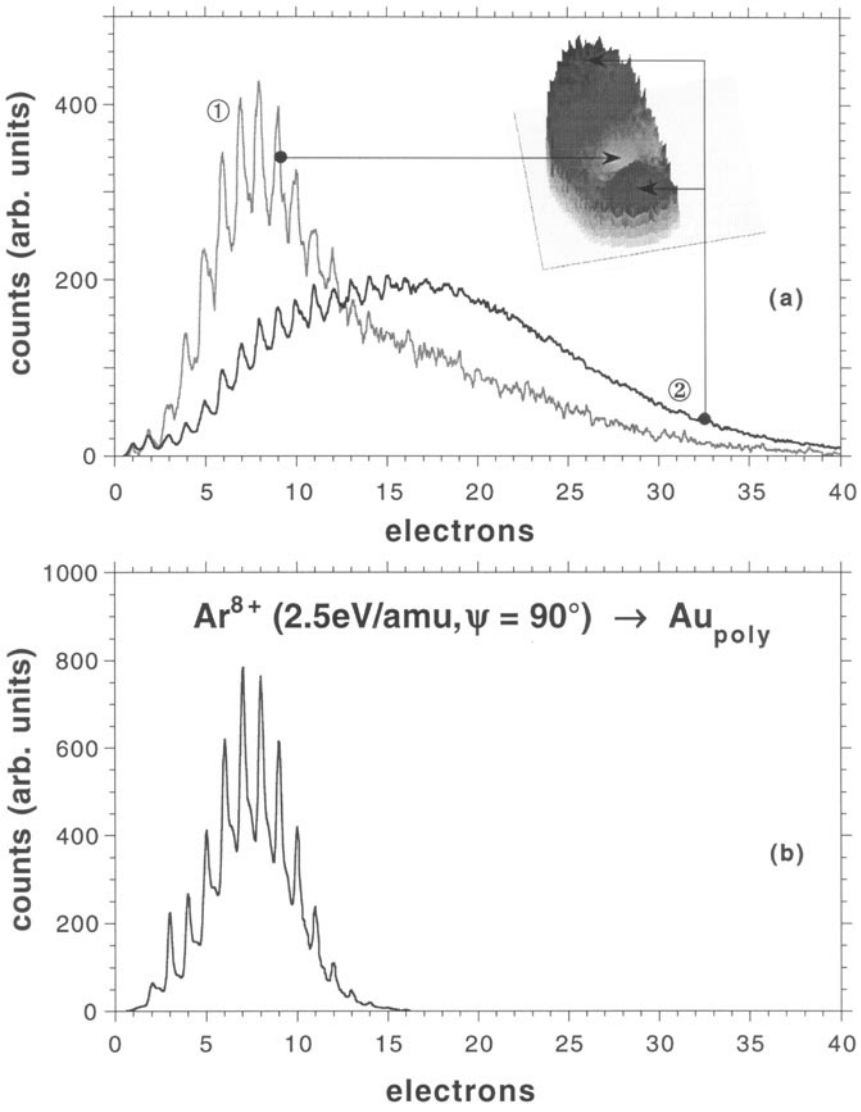


**Figure 14.** (*a*) Electron multiplicity spectra for the case of 0.45 keV $amu^{-1}$ $Ar^{8+}$ ions impinging under a grazing angle of 5° onto a Au(111) single crystal surface measured in coincidence with the central part (1) and with the wings (2) of the scattering distribution; see inset (Lemell *et al* 1998). (*b*) ES spectrum obtained for 2.5 eV $amu^{-1}$ normal incidence $Ar^{8+}$ projectiles on polycrystalline Au (Kurz *et al* 1992).

can be accommodated by the excitation energy being rapidly dissipated in the target material without inducing any structural modification. In recent studies on slow HCI impact on certain insulator surfaces a quite dramatic increase of the yields for total sputtering and secondary ion emission with increasing $q$ has been observed (Neidhart *et al* 1995a, Sporn *et al* 1997). Figure 15 shows total sputtering yields versus $q$ for a polycrystalline LiF target bombarded by $Ar^{q+}$ and $Xe^{q+}$ ions. Two competing models have been developed for this peculiar 'potential sputtering of insulators' (PSI), which explain the observed effects by 'Coulomb explosion' (CE)

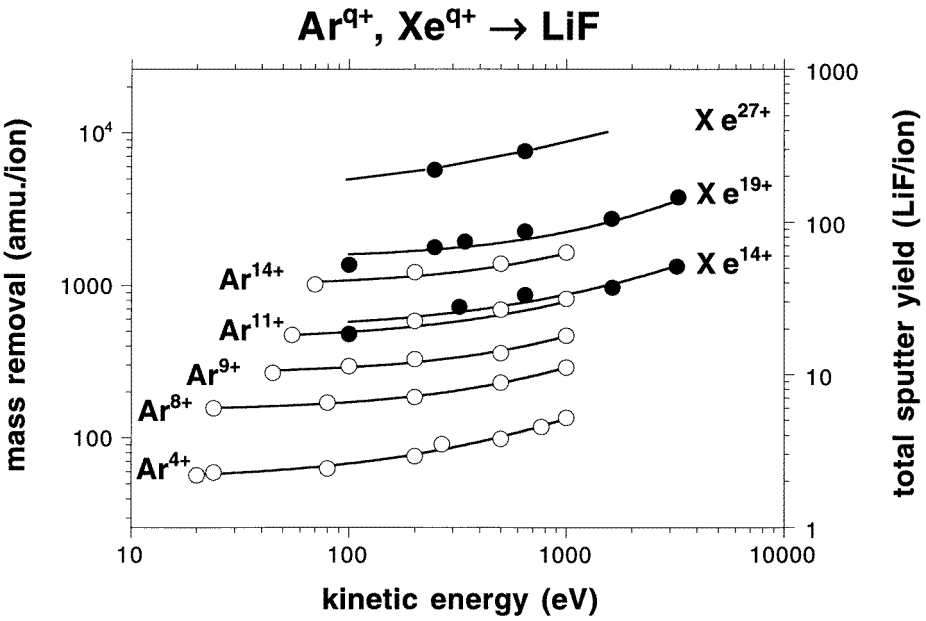


**Figure 15.** Mass removal for LiF in atomic mass units (left scale), and number of sputtered LiF molecules (right scale) per incident $Ar^{q+}$ (open symbols) and $Xe^{q+}$ (full symbols) as a function of impact energy (Sporn *et al* 1997).

and 'defect-mediated sputtering' (DS), respectively. In the CE model proposed by Bitenskii *et al* (1979), neutralization of a HCI impinging on an insulator surface is assumed to cause strong rapid electron depletion of the near-surface region. Mutual Coulomb repulsion of the remaining target ion cores will give rise to ejection of secondary ions from the positively charged surface domains, and shock waves generated by CE can ablate further target material (emission of neutral target atoms or clusters). In the different in principle DS approach, PSI is explained by defects produced in the course of electron capture by the HCI (Neidhart *et al* 1995a, Sporn *et al* 1997). In certain insulator materials (e.g. alkali halides and $SiO_2$) electronic defects can be induced by bombardment with energetic electrons or UV photons (electron- and photon-stimulated desorption: Green 1987, Walkup *et al* 1987, Szymonski *et al* 1992, Seifert *et al* 1993, Szymonski 1993). The interaction of a HCI with any target surface will result in electronic holes in the valence band and also electron–hole pair production.

Due to the strong electron–phonon coupling (i.e. efficient energy transfer from excited electrons to the phonon system of the solid) in alkali halides and $SiO_2$, an electronic excitation of the valence band can become localized by formation of 'self-trapped excitons' (STE) and/or 'self-trapped holes' (STH), which then will decay into different 'colour centres' and thus cause desorption of the neutralized anions (halides and oxygen). The neutral cations also produced will either be evaporated (as in the case of heated alkali halide samples) or removed from the insulator surface by momentum transfer from impinging projectiles. According to this DS model PSI cannot occur for any insulator, since enhanced sputter yields for higher HCI charge are only possible for targets involving strong electron–phonon coupling which keeps the electronic excitation produced by HCI impact localized via STE and/or STH formation, in full accordance with experimental observations (Varga *et al* 1997).

## 5. Outlook

The previous sections have shown that the main processes defining HA formation and decay upon impact of slow HCI on atomically clean metal surfaces are reasonably well understood as far as the situation up until close surface contact is concerned. The further development of these HA near the surface (in the selvedge) and inside the target bulk is not so well understood, and more studies are definitely needed, both on the experimental and theoretical side, to improve this situation. A promising experimental approach consists of coincidence studies for scattered projectiles and emitted electrons (both slow and fast) or x-ray photons, as then the projectile trajectories in the near-surface region can be reasonably well defined (see section 4.4), which is of value for the comparison with related calculations.

More work would also be desirable on HA formation at insulator surfaces. Briand *et al* (1997) performed measurements on Ar K x-ray emission induced by impact of $Ar^{17+}$ on H-terminated Si(111). At low impact velocity determined by the projectile image-charge acceleration, these authors claim to have found evidence for reflected, non-neutralized ions which have made no close surface contact ('trampoline effect'). These observations have been explained by the build-up of positive charge at the surface due to multiple RN and the consequent termination of further projectile approach. On the other hand, experiments on grazing incidence of HCI at insulator surfaces (Auth and Winter 1996) showed no characteristic differences to results from similar studies involving metal surfaces.

Another field of interest has recently been opened by attempts to produce 'free' HA or 'hollow ions'. By passing 30 keV $N^{6+}$ ions through Ni microcapillary foils (thickness of 1.5 $\mu$m, channel diameter 250 nm), Ninomiya *et al* (1997) detected K x-rays from N projectiles which have just left the foil. According to these measurements, about 1% of the primary $N^{6+}$ ions can pick up at least one electron from the microcapillary walls, and there is evidence that some of the hollow atoms and ions thereby produced have unexpectedly long lifetimes (up to ns).

A different approach for producing hollow atoms or ions might utilize RN from metal clusters or fullerenes into HCI. Jin *et al* (1996) demonstrated that up to nine-times charged fullerene ions can be produced in this way, while Martin *et al* (1998) showed that up to 60 electrons can be transiently captured (with 45 being emitted and 15 stabilized onto the projectile) in a collision between $Xe^{25+}$ and $C_{60}$.

No detailed investigation has been made on the configuration of the post-collisional projectiles which could probably exist in multi-excited states for some time after the collision.

Finally, 'potential sputtering of insulators' (PSI, see section 4.5) definitely deserves further attention. Related experiments should be made for insulator surfaces other than alkali halides, and for far higher primary ion charge states than so far applied. Of special interest are conceivable technical applications of PSI such as, e.g., the production of nanostructures on insulator surfaces by slow HCI treatment.

## Acknowledgments

This work has been supported by Austrian Fonds zur Förderung der wissenschaftlichen Forschung and Jubiläumsfonds der Österreichischen Nationalbank, and was carried out within Association EURATOM-ÖAW. The authors thank J Burgdörfer (TU Wien) for many valuable discussions and suggestions to improve the present manuscript. Fruitful collaborations with P Varga (TU Wien), M Delaunay (Grenoble), R Morgenstern (Groningen), N Stolterfoht (HMI Berlin), D Schneider (LLNL), and participation of G Lakits, H Kurz, K Töglhofer, M Vana, T Neidhart, M Sporn, C Lemell and H Eder in various parts of the measurements described in section 4 are gratefully acknowledged.

## References


Andrä H J 1988 *NATO Summer School on Fundamental Processes of Atomic Dynamics* (New York: Plenum)

——1989 *NATO Summer School on Atomic Physics of Highly Charged Ions* ed E Marrus (New York: Plenum)

Andrä H J *et al* 1991 *Proc. XVII Int. Conf. on Physics of Electronic and Atomic Collisions* ed MacGillivray *et al* (Brisbane: IOP Conference Proceedings) p 89

Apell P 1987 *Nucl. Instrum. Methods* B **23** 242

Arifov U A, Mukhamadiev E S, Parilis E S and Pasyuk A S 1973 *Sov. Phys.–Tech. Phys.* **18** 240

Arnau A, Zeijlmans van Emmichoven P A, Juaristi J I and Zaremba E 1995 *Nucl. Instrum. Methods* B **100** 279

Arnau A *et al* 1997 *Surf. Sci. Rep.* **229** 1

Aumayr F, Kurz H, Schneider D, Briere M A, McDonald J W, Cunningham C E and Winter HP 1993 *Phys. Rev. Lett.* **71** 1943

Aumayr F and Winter HP 1994 *Comment. At. Mol. Phys.* **29** 275

Aumayr F, Winter HP, Limburg J, Hoekstra R and Morgenstern R 1997 *Phys. Rev. Lett.* **79** 2590

Auth C and Winter H 1996 *Phys. Lett.* A **217** 119

Barany A and Setterlind C J 1995 *Nucl. Instrum. Methods* B **98** 184

Barany A *et al* 1985 *Nucl. Instrum. Methods* B **9** 397

Bardsley J N and Penetrante B M 1991 *Comment At. Mol. Phys.* **27** 43

Benninghoven A, Nihei Y, Shimizu R and Werner H W (ed) 1994 *Secondary Ion Mass Spectrometry (SIMS IX)* (New York: Wiley)

Bethe H A and Salpeter E E 1957 *Quantum Mechanics of One and Two Electron Systems* (New York: Academic)

Betz G and Wien K 1994 *Int. J. Mass Spectrom. Ion Proc.* **140** 1

Bitenskii I S, Murakhmetov M N and Parilis E S 1979 *Sov. Phys.–Tech. Phys.* **24** 618

Bitensky I S and Parilis E S 1989 *J. Physique* C **2** 227

Briand J P, de Billy L, Charles P, Essabaa S, Briand P, Geller R, Desclaux J P, Bliman S and Ristori C 1990 *Phys. Rev. Lett.* **65** 159

Briand J P, Thuriez S, Giardino G, Borsoni G, Froment M, Eddrief M and Sebenne C 1996 *Phys. Rev. Lett.* **77** 1452

Briand J P *et al Phys. Rev.* A **55** R2523

Burgdörfer J 1993 *Fundamental Processes and Applications of Atoms and Ions* ed C D Lin (Singapore: World Scientific)

Burgdörfer J, Kupfer E and Gabriel H 1987 *Phys. Rev.* A **35** 4963

Burgdörfer J, Lerner P and Meyer F W 1991 *Phys. Rev.* A **44** 5647

Burgdörfer J and Meyer F W 1993 *Phys. Rev.* A **47** R20

Burgdörfer J, Reinhold C and Meyer F 1995 *Nucl. Instrum. Methods* B **98** 415

Cobas A and Lamb W E 1944 *Phys. Rev.* **65** 327

Das J and Morgenstern R 1993 *Comment. At. Mol. Phys.* **29** 205

de Zwart S T 1987 *PhD Thesis* University of Groningen

de Zwart S T, Drentje A G, Boers A L and Morgenstern R 1989 *Surf. Sci.* **217** 298

de Zwart S T, Fried T, Boerma D O, Hoekstra R, Drentje A G and Boers A L 1986 *Surf. Sci.* **177** L939

de Zwart S T, Fried T, Jellen U, Boers A L and Drentje A G 1985 *J. Phys. B: At. Mol. Opt. Phys.* **18** L623

Delaunay M, Fehringer M, Geller R, Hitz D, Varga P and Winter HP 1985 *Proc. XIV Int. Conf. on Physics of Electronic and Atomic Collisions Conf. (Palo Alto, CA)* ed M J Coggiola *et al* p 477

——1987a *Phys. Rev.* B **35** 4232

Delaunay M, Fehringer M, Geller R, Varga P and Winter HP 1987b *Europhys. Lett.* **4** 377

Diez Muino R, Arnau A and Echenique P 1995 *Nucl. Instrum. Methods* B **98** 420

Diez Muino R, Stolterfoht N, Arnau A, Salin A and Echenique P 1996 *Phys. Rev. Lett.* **76** 4636

Diez Muino R, Salin A, Stolterfoht N, Arnau A and Echenique P 1998 *Phys. Rev.* A **57** 1126

Donets E D 1983 *Phys. Scr.* T **3** 11

——1985 *Nucl. Instrum. Methods* B **9** 522

Eder H, Aumayr F and Winter H 1999 *Nucl. Instrum. Methods* B at press

Fano U and Lichten W 1965 *Phys. Rev. Lett.* **14** 627

Folkerts L, Schippers S, Zehner D M and Meyer F W 1995 *Phys. Rev. Lett.* **74** 2204

Green T 1987 *Phys. Rev.* B **35** 781

Hägg L, Reinhold C O and Burgdörfer J 1997 *Phys. Rev.* A **55** 2097

——1998 *Photonic, Electronic and Atomic Collisions* ed F Aumayr and H P Winter (Singapore: World Scientific) p 683

Hagstrum H D 1953 *Phys. Rev.* **91** 543

——1954a *Phys. Rev.* **96** 325

——1954b *Phys. Rev.* **96** 336
——1956 *Phys. Rev.* **104** 672
Hagstrum H D and Becker G E 1973 *Phys. Rev.* B **8** 107
Hasselkamp D 1992 *Particle Induced Electron Emission II (Springer Tracts in Modern Physics vol 123)* (Heidelberg: Springer) p 1
Jin J, Khemliche H, Prior M H and Xie Z 1996 *Phys. Rev.* A **53** 615
Khemliche H, Schlathoelter T, Hoekstra R, Morgenstern R and Schippers S 1998 *Phys. Rev. Lett.* **81** 1219
Kiernan L *et al* 1994 *Phys. Rev. Lett.* **72** 2359
Köhrbrück R, Grether M, Spieler A, Stolterfoht N, Page R, Saal A and Bleck-Neuhaus J 1994 *Phys. Rev.* A **50** 1429
Kurz H, Aumayr F, Lemell C, Töglhofer K and Winter HP 1993a *Phys. Rev.* A **48** 2182
——1993b *Phys. Rev.* A **48** 2192
Kurz H, Aumayr F, Schneider D, Briere M A, McDonald J W and Winter HP 1994 *Phys. Rev.* A **49** 4693
Kurz H, Töglhofer K, Winter HP, Aumayr F and Mann R 1992 *Phys. Rev. Lett.* **69** 1140
Lakits G, Aumayr F and Winter HP 1989 *Rev. Sci. Instrum.* **60** 3151
Lakits G, Aumayr F, Heim M and Winter HP 1990 *Phys. Rev.* A **42** 5780
Lemell C, Stöckl J, Burgdörfer J, Betz G, Winter HP and Aumayr F 1998 *Phys. Rev. Lett.* **81** 1965
Lemell C, Winter HP, Aumayr F, Burgdörfer J and Meyer F W 1996 *Phys. Rev.* A **53** 880
Lemell C, Winter HP, Aumayr F, Burgdörfer J and Reinhold C 1995 *Nucl. Instrum. Methods* B **102** 33
Limburg J, Das J, Schippers S, Hoekstra R and Morgenstern R 1994 *Phys. Rev. Lett.* **73** 786
Limburg J, Schippers S, Hoekstra R, Morgenstern R, Kurz H, Aumayr F and Winter HP 1995b *Phys. Rev. Lett.* **75** 217
Limburg J, Schippers S, Hughes I, Hoekstra R, Morgenstern R, Hustedt S, Hatke N and Heiland W 1995a *Nucl. Instrum. Methods* B **98** 436
——1995a *Phys. Rev.* A **51** 3873
Martin S, Chen L, Denis A and Desesquelles J 1998 *Phys. Rev.* A **57** 4518
Mau Chen 1990 *Tabulated Ionisation Potentials* (Lawrence Livermore Natl Lab.) private communication
Massey H S W 1930 *Proc. Camb. Phil. Soc.* **26** 386
——1931 *Proc. Camb. Phil. Soc.* **27** 469
Melin G and Girard A 1997 *Accelerator Based Atomic Physics–Techniques and Applications* ed S M Shafroth and J Austin (New York: AIP) ch 2
Meyer F W, Folkerts L, Folkerts H O and Schippers S 1995 *Nucl. Instrum. Methods* B **98** 441
Meyer F W, Overbury S H, Havener C C, Zeijlmans van Emmichhoven P A, Burgdörfer J and Zehner D M 1991a *Phys. Rev.* A **44** 7214
Meyer F W, Overbury S H, Havener C C, Zeijlmans van Emmichhoven P A and Zehner D M 1991b *Phys. Rev. Lett.* **67** 723
Morgenstern R and Das J 1994 *Europhys. News* **25** 3
Moribayashi K, Sasaki A and Tajima T 1998 *Phys. Rev.* A **58** 2007
Neidhart T, Pichler F, Aumayr F, Winter HP, Schmid M and Varga P 1995a *Phys. Rev. Lett.* **74** 5280
——1995b *Nucl. Instrum. Methods* B **98** 465
——1995c *Proc. 3S'95 Symp. Surface Science* ed P Varga and F Aumayr (Kitzsteinhorn, Salzburg, Austria) p 74
Niehaus A 1986 *J. Phys. B: At. Mol. Phys.* **19** 2925
Ninomiya S, Yamazaki Y, Koike F, Masuda H, Azuma T, Komaki K, Kuroki K and Sekiguchi M 1997 *Phys. Rev. Lett.* **78** 4557
Oliphant M L E and Moon P B 1930 *Proc. R. Soc.* A **127** 388
Ryufuku H, Sasaki K and Watanabe T 1980 *Phys. Rev.* A **21** 7451
Schippers S, Limburg J, Das J, Hoekstra R and Morgenstern R 1994 *Phys. Rev.* A **50** 540
Schneider D, Clark M W, Penetrante B, McDonald J, DeWitt D and Bardsley J N 1991 *Phys. Rev.* A **44** 3119
Seifert N, Liu D, Bernes A, Albridge R, Yan Q, Tolk N, Husinsky W and Betz G 1993 *Phys. Rev.* B **47** 7653
Shekter S S 1937 *J. Exp. Theor. Phys. (USSR)* **7** 750
Sigmund P (ed) 1993 *Fundamental Processes in Sputtering of Atoms and Molecules (SPUT 92, Copenhagen), Mat. Fys. Medd.* **43** 2
Snowdon K J, Havener C C, Meyer F W, Overbury S H, Zehner D M and Heiland W 1988 *Phys. Rev.* A **38** 2294
Sporn M, Libiseller G, Neidhart T, Schmid M, Aumayr F, Winter HP, Varga P, Grether M and Stolterfoht N 1997 *Phys. Rev. Lett.* **79** 945
Stöckli M P 1997 *Accelerator Based Atomic Physics–Techniques and Applications* ed S M Shafroth and J Austin (New York: AIP)
Stolterfoht N, Arnau A, Grether M, Köhrbrück R, Spieler A, Page R, Saal A, Thomaschewski J and Bleck-Neuhaus J 1995 *Phys. Rev.* A **52** 445
Stolterfoht N, Niemann D, Grether M, Spieler A, Arnau A, Lemell C, Aumayr F and Winter HP 1997 *Nucl. Instrum.*

*Methods* B **124** 303
Szymonski M 1993 *Fundamental Processes in Sputtering of Atoms and Molecules* (Copenhagen: Royal Danish Academy of Sciences) p 495
Szymonski M, Poradzisz A, Czuba P, Kolodziej J, Piatkowski P, Fine J, Tanovic L and Tanovic N 1992 *Surf. Sci.* **260** 295
Thomaschewski J, Bleck-Neuhaus J, Grether M, Spieler A and Stolterfoht N 1998 *Phys. Rev.* A **57** 3665
Vaeck N and Hansen J E 1995 *J. Phys. B: At. Mol. Opt. Phys.* **28** 3523
Vana M, Aumayr F, Lemell C and Winter HP 1995b *Int. J. Mass Spectrom. Ion Proc.* **149/150** 45
Vana M, Kurz H, Winter HP and Aumayr F 1995a *Nucl. Instrum. Methods* B **100** 402
Varga P and Diebold U 1994 *Low Energy Ion–Surface Interaction* (New York: Wiley)
Varga P, Neidhart T, Sporn M, Libiseller G, Schmid M, Aumayr F and Winter HP 1997 *Phys. Scr.* T **73** 307
Varga P and Winter HP 1992 *Particle Induced Electron Emission II (Springer Tracts in Modern Physics vol 123)* (Heidelberg: Springer) p 149
Walkup R E, Avouris P and Ghosh A 1987 *Phys. Rev.* B **36** 4577
Winecki S, Cocke C L, Fry D and Stöckli M P 1996 *Phys. Rev.* A **53** 4228
Winter H 1992 *Europhys. Lett.* **18** 207
Winter H, Auth C, Schuch R and Beebe E 1993 *Phys. Rev. Lett.* **71** 1939
Winter HP, Vana M, Lemell C and Aumayr F 1996 *Nucl. Instrum. Methods* B **115** 224
Yan Q and Meyer F W 1997 *Materials Science Forum* (Switzerland: Trans Tech. Publications) p 629
Zehner D M, Overbury S H, Havener C C, Meyer F W and Heiland W 1986 *Surf. Sci.* **178** 359